Research Article

Geochemistry of late Cenozoic lavas on Kunashir Island, Kurile Arc

ALEXEY Y. MARTYNOV,[1,*] JUN-ICHI KIMURA,[2] YURI A. MARTYNOV[1] AND ALEXSANDER V. RYBIN[3]

[1]*Far East Geological Institute, Far Eastern Branch of Russian Academy of Science, Vladivostok 690022, Russia (email: amartynov@lycos.com),* [2]*Institute for Research on Earth Evolution (IFREE), Japan Agency for Marine–Earth Science and Technology (JAMSTEC), 2-15 Natsushima-cho, Yokosuka 237-0061, Japan, and* [3]*Institute of Marine Geology and Geophysics, Far Eastern Branch of Russian Academy of Science, Yujno-Sakhalinsk 693022, Russia*

Abstract Middle Miocene to Quaternary lavas on Kunashir Island in the southern zone of the Kurile Arc were examined for major, trace, and Sr–Nd–Pb isotope compositions. The lavas range from basalt through to rhyolite and the mafic lavas show typical oceanic island arc signatures without significant crustal or sub-continental lithosphere contamination. The lavas exhibit across-arc variation, with increasingly greater fluid-immobile incompatible element contents from the volcanic front to the rear-arc; this pattern, however, does not apply to some other incompatible elements such as B, Sb, and halogens. All Sr–Nd–Pb isotope compositions reflect a depleted source with Indian Ocean mantle domain characteristics. The Nd and Pb isotope ratios are radiogenic in the volcanic front, whereas Sr isotope ratios are less radiogenic. These Nd isotope ratios covary with incompatible element ratios such as Th/Nd and Nb/Zr, indicating involvement of a slab-derived sediment component by addition of melt or supercritical fluid capable of mobilizing these high field-strength elements and rare earth elements from the slab. Fluid mobile elements, such as Ba, are also elevated in all basalt suites, suggesting involvement of slab fluid derived from altered oceanic crust. The Kurile Arc lavas are thus affected both by slab sediment and altered basaltic crust components. This magma plumbing system has been continuously active from the Middle Miocene to the present.

Key words: across-arc variation, incompatible element, Indian Ocean mantle, Kurile Arc, late Cenozoic, Sr–Nd–Pb isotopes.

INTRODUCTION

Although numerous studies of arc magmatism have been made, details of the initiation, development, and establishment of subduction zone magmatism remain unsolved issues for many arcs (Stern 2004). For example, arc initiation can only be investigated in a limited number of arcs such as the Izu–Bonin and Mariana systems (Stern & Bloomer 1992; Ishizuka *et al.* 2006a). Back arc basin (BAB) openings share a common feature in the course of volcanic arc development (e.g. Stern & Bloomer 1992) and BAB opening related volcanism have also remained poorly investigated until recent years (Taylor & Martinez 2003; Kelley *et al.* 2006).

The northeast Japan and Kurile Arcs developed at the eastern margin of the Eurasia continent (Fig. 1), and are associated with the BAB of the Sea of Japan and the Kurile Basin, which formed in the late Cenozoic (Tamaki *et al.* 1992; Kimura 1996; Baranov *et al.* 2002). These arcs have been studied intensively in terms of BAB opening and subsequent arc magmatism (Pouclet & Bellon 1992; Goto *et al.* 1995; Nakajima *et al.* 1995; Okamura *et al.* 1995, 1998, 2005; Pouclet *et al.* 1994; Yoshida *et al.* 1995; Takagi *et al.* 1999; Yoshida 2001; Shuto *et al.* 2004, 2006; Kimura &

*Correspondence.

Received 9 April 2008; accepted for publication 25 December 2008.

doi:10.1111/j.1440-1738.2009.00684.x

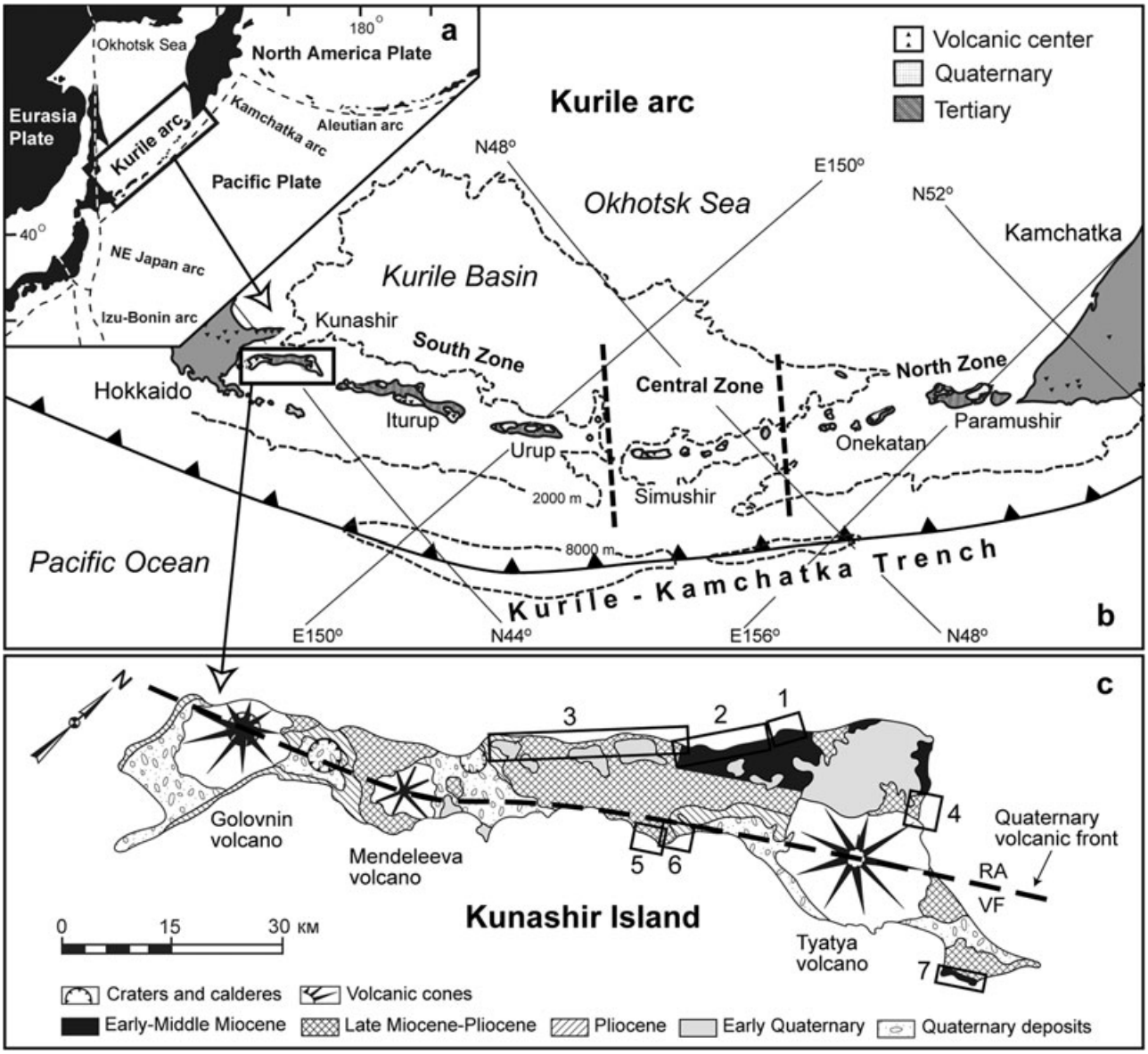

Fig. 1 Map (a) of Kurile Island Arc with (b) locations of Quaternary active volcanoes (after Bailey *et al.* 1989). (c) Schematic geological map of Kunashir Island (modified after Fedorchenko *et al.* 1989) with location of Quaternary volcanic front (thick broken line). Open rectangles with numbers are sample localities: 1, Kompressornii–Prasolova; 2, Prasolovo–Nazarovo; 3, Nazarovo–Lagunnoe Bay; 4, Ekaterina Volcano; 5, Filatova Bay; 6, Mostovaya–Filatova Bay; 7, Lovtsova peninsula. Samples from these localities are shown in Table 1.

Yoshida 2006; Sato *et al.* 2007), because volcanic rocks of these stages are exposed on land due to subsequent uplift within the arc. Across-arc geochemical variation of these arcs appears to have developed since the Pliocene (Ryan *et al.* 1995; Yoshida *et al.* 1995; Yoshida 2001). Typical magmatic arcs with characteristic across-arc geochemical variations (Gill 1981; Pearce & Parkinson 1993; Peate & Pearce 1998) were established in the early Quaternary (Shibata & Nakamura 1997; Kimura & Yoshida 2006).

Although numerous geochronological and geochemical data are available for the west Kurile (Hokkaido) and northeast Japan Arcs, with the exception of the Quaternary lavas (Bailey *et al.* 1989; Ishikawa & Tera 1997; Bindeman & Bailey 1999), the late Cenozoic lavas in the main part of the Kurile Arc (between Kunashir and Kamchatka Islands; Fig. 1b) have been poorly investigated. Miocene to Quaternary volcanic rocks occur, but the Miocene volcanics have not yet been subjected to comprehensive petrological or geochemical study. Existing studies are sparse. Geophysical, geological, petrographic, and petrochemical data in the Kurile Arc were first summarized by Gorshkov (1967). Syvorotkin and Rusinova (1989)

pointed out the depleted nature of the late Pliocene basalts, and related these to the formation of the Kurile Basin.

Published trace element and isotopic data are available only for limited Quaternary Volcanoes and adjacent submarine volcanic rocks in the Kurile Basin (Zhuravlev *et al.* 1985; Bailey *et al.* 1989; Ishikawa & Tera 1997; Bindeman & Bailey 1999; Martynov *et al.* 2005). Many of these studies have dealt with limited or specific elements or isotopes, such as B, Nb, Sb, and B isotopes, and thus, comprehensive datasets including major, trace, and Sr–Nd–Pb isotope compositions are rare. Moreover, the Kurile Arc is underlain by volcanic rocks dating back to the middle Miocene, and the geochemistry of these rocks is very poorly known. These older volcanic rocks may have formed during the opening of the BAB Kurile Basin (Baranov *et al.* 2002), and the development history of the basin may thus be similar to that in the adjacent Hokkaido or northeast Japan Arcs. This paper provides the first comprehensive set of major, trace, and Sr–Nd–Pb isotope analyses of the Miocene to Quaternary volcanic rocks on Kunashir Island in the South Zone of the Kurile Arc (Fig. 1b), and discusses the magmatic arc origin.

GEOLOGICAL BACKGROUND

The Kurile Arc forms part of the geodynamic system where the Pacific Plate subducts beneath the North American Plate. The Kurile Arc consists of the Kurile–Kamchatka Trench, the Big Kurile volcanic chain, and the Kurile Basin in the rear-arc (Fig. 1b).

Formation of the Kurile volcanic chain began in the Early Miocene or in the Oligocene. The total length of the volcanic zone exceeds 1150 km, and its width ranges from 100 to 200 km. The depth of the submerged oceanic Pacific Plate slab beneath the volcanic chain varies between 94.2 km for North Kurile and 92 km for South Kurile (Syracuse & Albers 2006). The thickness of the crust varies only slightly along the arc, being 28–33 km in the South Zone, 25–30 km in the central zone, and 32–36 km in the North Zone (Zlobin *et al.* 1987). The presence of abundant metamorphic rock xenoliths (plagioclase–pyroxene granulites, amphibolite, hornfels, different types of schists) in the Quaternary basalts provides evidence for the formation of the Kurile Arc on a continental crust (Fedorchenko *et al.* 1989).

The Kurile Basin was formed by back-arc spreading (Baranov *et al.* 2002). On the basis of heat flow data, basement depth, and seismostratigraphy, the basin is thought to have formed in Early Oligocene to Middle Miocene time (32–15 Ma) (Baranov *et al.* 2002). Although spreading switched to compression since the early Pliocene, the magmatic process in the Kurile Basin remains active until present time. This is evidenced by high heat flow (up to 105 mW/m^2) and the presence of Quaternary (0.84–1.07 Ma) submarine volcanoes in the eastern Kurile Basin (Tararin *et al.* 2000; Baranov *et al.* 2002).

STRATIGRAPHY OF VOLCANIC ROCKS ON KUNASHIR ISLAND

As outlined above, volcanic activity on the Kurile Islands began in the Early Miocene or Oligocene. The activity produced four volcanigenic chronological units: the Greentuff Formation (Middle Miocene), Volcanic–Diatomaceous–Chert Formation (Late Miocene), Basaltic Formation (Pliocene), and Andesitic Formation (Quaternary) (Piskunov 1987).

The Greentuff Formation consists of volcanigenic materials with a total thickness of about 4000 m. On Kunashir Island (Fig. 1c) this formation is represented by the Kunashirskaya and Lovtsovskaya Members (shown as Early–Middle Miocene in Fig. 1c). The Kunashirskaya Member is essentially volcanigenic in nature, consisting of volcanic breccias of basaltic, intermediate, and felsic composition, with interbeds or lenses of tuffs, volcanigenic sandstones, and occasional conglomerates. The Lovtsovskaya Member is about 1500 m thick. Volcanigenic conglomerates and breccias alternating with siltstones and poorly sorted sandstones form the base of the member. Rhythmic interbedding of tuffs, sandstones, siltstones, and, to a lesser extent, tuff–diatomites are observed.

The Volcanic–Diatomaceous–Chert Formation on Kunashir Island (shown as Late Miocene–Pliocene in Fig. 1c) is represented by the Alekhinskaya and Golovninskaya Members (Piskunov 1987). These have a total thickness of about 1500 m, and consist of basal conglomerates and conglomerate–breccias. Layered beds composed of 0.2- to 4-m-thick andesite or dacite tuffs, Volcanogenic sandstones, breccias, and diatomites and siltstones overlie the basal conglomerates.

The Basaltic Formation occurs almost on all islands including Kunashir. On Kunashir Island the

formation is represented by strata consisting of lava flows of 5 to 50 m thick in basaltic, basaltic andesite, and andesite compositions (shown as Pliocene in Fig. 1c). These lavas alternate with tuffs and reworked conglomerate to breccias and sandstones. The total thickness of the formation is about 400 m.

The Andesitic Formation forms the basement of Quaternary to modern volcanic edifices (Piskunov 1987; shown as Early Quaternary and volcanic cones in Fig. 1c). As its name implies, this formation is composed predominantly of andesites.

SAMPLES AND ANALYTICAL METHODS

Major and trace element compositions of 70 samples were determined by X-ray fluorescence spectrometry (XRF) using glass disks prepared with an alkali flux. Powdered samples were ignited in a muffle furnace for three hours at 1000°C to obtain loss on ignition (LOI). The alkali flux used is a mixture of lithium tetraborate and lithium metaborate with a mixing ratio of 4:1. The glass disks were prepared by mixing 1.8 g of sample powder and 3.6 g of the alkali flux before fusion in an automated bead sampler (Kimura & Yamada 1996). The resulting glass disks were analyzed for 10 major elements and 14 trace elements using a Rigaku RIX 2000 spectrometer at Shimane University (Matsue, Shimane, Japan). Analytical uncertainties by XRF are less than 2% for all major elements with concentrations greater than 1 wt% and less than 10% for most of the trace elements with concentrations greater than 5 ppm (Kimura & Yamada 1996). The XRF and LOI results are presented in Table 1.

Sixteen selected samples were analyzed for additional trace and ultra-trace elements using solution-based inductively coupled plasma–mass spectrometry (ICP-MS) (Kimura *et al.* 1995). The ICP-MS used was a Thermo Elemental VG PQ3 at Shimane University. Analytical precision for the ICP-MS analysis is less than 2% for most elements with concentrations greater than 1 ppm, and external accuracy is better than 6%, based on replicate analyses of JB-1 and JB-2 basalt standards provided by the Geological Survey of Japan (Kimura *et al.* 1995).

Sr, Nd, and Pb isotope analyses of 12 basaltic rocks were made at Shimane University using a multiple-collector ICP-MS (Thermo Elemental VG Plasma 54). The reagents used were ultra-pure hydrofluoric, nitric, hydrochloric, and hydrobromic acids. Element separation procedures for Sr, Nd, and Pb follow Iizumi *et al.* (1994, 1995) and Kimura *et al.* (2003). Standard samples analyzed with the unknowns yielded the isotope ratios $^{87}Sr/^{86}Sr = 0.702151 \pm 0.000015$ for SRM 987 and 0.703796 ± 0.000014 for JB-2; $^{143}Nd/^{144}Nd = 0.511853 \pm 0.000010$ for La Jolla and $^{143}Nd/^{144}Nd = 0.513097 \pm 0.000010$ for JB-2; $^{206}Pb/^{204}Pb = 16.9412 \pm 0.0008$, $^{207}Pb/^{204}Pb = 15.4996 \pm 0.0011$, and $^{208}Pb/^{204}Pb = 36.7252 \pm 0.0026$ for SRM981; and $^{206}Pb/^{204}Pb = 18.3447 \pm 0.0008$, $^{207}Pb/^{204}Pb = 15.5660 \pm 0.0008$, and $^{208}Pb/^{204}Pb = 38.2866 \pm 0.0031$ for JB-2. Analytical precisions for the unknowns are similar to those for the standards. Trace element and isotope data are given in Table 2.

MAJOR AND TRACE ELEMENT CHARACTERISTICS

According to geological observations (Baranov *et al.* 2002), lavas from the Miocene or Pliocene strata are subaqueous eruptives. Some exhibit high LOI, suggesting alteration (Table 1), but most have LOI less than 3 wt%. The possible effects of alteration were also assessed by examining Na_2O/K_2O ratios. All but four samples had Na_2O/K_2O less than 20 (Table 1), indicating that alkali earth element re-mobilization was minimal for the low Na_2O/K_2O samples (Miyashiro 1974). No systematic correlation between LOI and fluid mobile elements such as K_2O, Rb, and Ba is evident (not shown). We therefore conclude that re-mobilization of elements is minimal in most of the subaqueous samples. Consequently, hereafter we use all elements in examination of across-arc variation. However, a more stringent choice of elements has been used for examination of magma sources in later sections.

We have examined across the arc variation of the volcanic rocks in different ages. The present day position of the Wadati–Benioff zone is estimated to lie at a depth of about 92 km beneath the volcanic front of South Kurile (Syracuse & Albers 2006) and the depth contours are parallel to the elongation axis of Kunashir Island. However, it is not possible to determine the depths of the Wadati–Benioff zone in the geological past. Therefore, we classify lava samples older than Quaternary based on their physiographical distribution. The lava samples collected from the forearc side of the Quaternary volcanic front are classified as volcanic front (VF) samples whereas the others are classified as rear-arc (RA) samples (VF/RA shown in Fig. 1c). These

Table 1 Major and trace element composition of Kunashir lavas

Sample No.	Location	Age	Suite	SiO_2	TiO_2	Al_2O_3	Fe_2O_3	MnO	MgO	CaO	Na_2O	K_2O	P_2O_5	Total	LOI	Na_2O/K_2O
				[Major elements in wt%]												
P-127/3	Kompressornii–Prasolova	Mid Miocene	RA	50.94	1.06	19.17	9.51	0.40	7.24	9.65	2.23	0.18	0.11	100.50	5.70	12.1
P-127/6	Kompressornii–Prasolova	Mid Miocene	RA	51.26	0.95	18.95	10.06	0.16	6.22	8.88	2.41	0.71	0.09	99.70	2.54	3.4
P-152/1	Orlovskii Ness	Mid Miocene	RA	73.78	0.42	14.19	3.00	0.04	0.78	2.95	3.72	1.22	0.06	100.14	2.03	3.1
P-174/4	Prasolovo–Nazarovo	Mid Miocene	RA	55.28	0.53	16.60	8.58	0.16	6.49	6.03	4.11	0.53	0.04	98.36	2.30	7.8
P-33/2	Prasolovo–Nazarovo	Mid Miocene	RA	44.56	1.15	20.99	13.79	0.23	6.48	9.00	2.05	0.08	0.13	98.46	7.23	27.1
P-74/4	Kompressornii–Prasolova	Mid Miocene	RA	52.22	0.96	19.42	10.65	0.06	10.07	3.65	3.34	0.44	0.02	100.85	6.08	7.6
P-75/13	Nazarovo–Lagunnoe Bay	Mid Miocene	RA	52.50	0.56	14.62	9.75	0.38	12.22	8.27	1.35	1.11	0.06	100.82	1.85	1.2
P-82/2	Prasolovo–Nazarovo	Mid Miocene	RA	57.60	0.80	16.72	9.05	0.16	4.05	7.79	2.55	0.83	0.09	99.63	0.32	3.1
P-82/3	Prasolovo–Nazarovo	Mid Miocene	RA	54.13	1.50	16.11	12.26	0.28	4.97	6.34	3.21	0.18	0.18	99.16	6.94	17.4
P-82/4	Prasolovo–Nazarovo	Mid Miocene	RA	54.97	0.98	16.75	11.01	0.23	5.60	7.60	2.45	0.28	0.13	100.01	2.92	8.7
P-61/4	Lovtsova peninsula	Mid Miocene	VF	53.25	0.98	17.25	12.22	0.14	6.16	5.96	2.45	0.63	0.03	99.07	9.68	3.9
P-54/2	Filatova Bay	Mid Miocene	VF	73.18	0.42	13.91	3.71	0.11	0.82	3.46	3.94	0.36	0.07	99.99	0.50	10.9
P-otp	Filatova Bay	Mid Miocene	VF	77.07	0.26	13.56	1.91	0.02	0.56	1.77	4.92	0.18	0.02	100.27	0.64	26.7
P-124/12	Ekaterina Volcano	Upper Miocene	RA	55.45	0.88	17.52	8.89	0.24	4.47	8.40	2.92	0.75	0.14	99.65	3.28	3.9
P-129/11	Prasolovo–Nazarovo	Upper Miocene	RA	55.50	0.62	16.98	9.11	0.16	5.91	6.79	4.02	0.21	0.05	99.36	1.65	18.8
P-135/10	Nazarovo–Lagunnoe Bay	Upper Miocene	RA	50.14	1.14	18.52	11.50	0.29	3.93	11.06	2.62	0.72	0.06	99.98	0.67	3.6
P-135/6	Nazarovo–Lagunnoe Bay	Upper Miocene	RA	68.49	0.67	15.42	5.48	0.22	2.34	3.06	2.78	1.82	0.17	100.44	3.71	1.5
P-136/16	Nazarovo–Lagunnoe Bay	Upper Miocene	RA	60.81	0.88	14.66	8.58	0.14	4.17	6.58	2.61	0.87	0.12	99.42	1.36	3.0
P-138/2	Nazarovo–Lagunnoe Bay	Upper Miocene	RA	64.91	0.63	17.12	5.74	0.07	1.83	5.59	3.44	1.02	0.13	100.47	1.86	3.4
P-70/1	Ekaterina Volcano	Upper Miocene	RA	54.00	1.03	19.48	9.10	0.27	4.06	6.92	2.38	2.45	0.18	99.87	6.01	1.0
P-71/3	Ekaterina Volcano	Upper Miocene	RA	51.87	0.84	18.96	10.09	0.19	5.12	7.32	3.65	0.87	0.11	99.02	7.03	4.2
P-75/10	Kompressornii–Prasolova	Upper Miocene	RA	57.02	0.92	17.15	9.11	0.16	3.93	8.09	2.66	1.23	0.14	100.40	1.60	2.2
P-75/7	Kompressornii–Prasolova	Upper Miocene	RA	60.79	0.76	16.42	7.63	0.15	2.94	6.46	3.00	1.32	0.10	99.57	2.01	2.3
P-82/6	Nazarovo–Lagunnoe Bay	Upper Miocene	RA	52.23	0.88	18.64	10.05	0.16	5.06	10.64	1.89	0.31	0.11	99.97	1.90	6.1
P-147/25	Filatova Bay	Upper Miocene	VF	53.66	1.28	15.47	12.17	0.27	4.86	7.73	2.80	0.52	0.30	99.06	3.90	5.4
P-148/8	Filatova Bay	Upper Miocene	VF	52.72	0.77	17.87	10.72	0.19	5.36	9.68	1.82	0.08	0.04	99.26	0.85	24.0
P-51/3	Filatova Bay	Upper Miocene	VF	74.54	0.59	13.83	2.90	0.11	0.50	3.36	3.91	0.40	0.09	100.23	0.60	9.7
P-78/3	Mendeleev Volcano	Upper Miocene	VF	70.98	0.45	14.79	4.70	0.09	1.38	3.97	3.78	0.27	0.07	100.47	1.07	14.0
P-120/8	Ekaterina Volcano	Pliocene	RA	53.60	1.01	19.00	8.77	0.17	4.16	9.16	3.03	0.44	0.18	99.51	1.85	6.9
P-121/2	Ekaterina Volcano	Pliocene	RA	49.53	0.95	17.26	9.10	0.16	5.29	13.74	1.93	0.53	0.84	99.32	0.98	3.6
P-122/1	Ekaterina Volcano	Pliocene	RA	57.28	1.01	16.24	9.50	0.18	3.53	7.83	2.81	0.62	0.20	99.21	2.54	4.5
P-68/3	Ekaterina Volcano	Pliocene	RA	50.15	1.12	17.94	9.19	0.15	5.27	12.51	2.31	0.51	0.26	99.40	2.51	4.6
P-69/10	Ekaterina Volcano	Pliocene	RA	52.89	1.04	20.44	8.46	0.11	6.15	6.27	3.78	0.46	0.18	99.78	5.29	8.3
P-69/7	Ekaterina Volcano	Pliocene	RA	60.56	1.01	15.83	7.97	0.15	2.93	5.58	3.29	1.87	0.21	99.39	2.12	1.8
P-11/2003	Mendeleev Volcano	Pliocene	VF	61.98	0.66	15.38	8.17	0.15	2.89	6.49	2.64	0.51	0.06	98.92	0.97	5.2
P-151/1	Mostovaya–Filatova Bay	Pliocene	VF	54.33	0.63	17.36	10.15	0.17	5.54	10.02	1.78	0.39	0.04	100.41	0.74	4.6
P-151/6	Mostovaya–Filatova Bay	Pliocene	VF	49.36	0.57	19.26	9.96	0.18	6.28	12.71	1.57	0.00	0.03	99.90	1.85	–

Table 1 *Continued*

Sample No.	Location	Age	Suite	SiO_2	TiO_2	Al_2O_3	Fe_2O_3	MnO	MgO	CaO	Na_2O	K_2O	P_2O_5	Total	LOI	Na_2O/K_2O
P-84/2	Mostovaya–Filatova Bay	Pliocene	VF	54.68	0.67	18.67	9.26	0.21	4.47	9.28	2.36	0.31	0.06	99.94	3.69	7.6
P-112/14	Nazarovo–Lagunnoe Bay	Quaternary	RA	48.95	0.59	14.89	11.14	0.17	12.68	10.07	1.23	0.06	0.04	99.83	–0.43	19.7
P-118/2000	Mendeleev Volcano	Quaternary	VF	62.83	0.66	17.82	6.52	0.10	1.11	6.82	3.08	0.54	0.10	99.57	1.18	5.8
P-191/2002	Mendeleev Volcano	Quaternary	VF	63.06	0.69	17.26	6.74	0.21	2.07	6.17	3.24	0.60	0.12	100.16	2.06	5.5
P-2/2003	Mendeleev Volcano	Quaternary	VF	65.00	1.01	14.19	7.98	0.15	1.64	5.36	3.35	0.82	0.15	99.64	0.14	4.1
P-202/2002	Mendeleev Volcano	Quaternary	VF	74.16	0.60	13.73	2.93	0.09	0.64	3.33	3.82	0.37	0.10	99.75	1.13	10.4
P-228/2001	Mendeleev Volcano	Quaternary	VF	64.97	0.98	15.01	7.63	0.12	1.38	5.03	3.26	0.79	0.13	99.28	2.58	4.1
P-241/2001	Mendeleev Volcano	Quaternary	VF	58.75	0.89	16.35	9.61	0.26	2.88	7.30	2.85	0.25	0.09	99.23	0.53	11.4
P-250/2001	Mendeleev Volcano	Quaternary	VF	61.58	0.90	19.70	8.37	0.25	1.59	4.74	2.57	0.36	0.12	100.18	0.18	7.2
P-258/2001	Mendeleev Volcano	Quaternary	VF	58.37	0.97	19.60	9.63	0.22	2.30	5.96	2.82	0.23	0.10	100.18	4.08	12.2
P-286/2001	Golovnin Volcano	Quaternary	VF	62.65	0.57	16.98	7.31	0.15	2.87	6.91	2.38	0.43	0.04	100.30	2.97	5.5
P-287/2001	Golovnin Volcano	Quaternary	VF	69.51	0.64	15.23	4.89	0.15	1.16	4.43	3.59	0.23	0.09	99.92	0.85	15.6
P-40/2000	Golovnin Volcano	Quaternary	VF	54.59	0.75	17.09	10.48	0.18	5.23	9.30	1.99	0.10	0.06	99.78	0.11	19.5
P-41/2000	Golovnin Volcano	Quaternary	VF	49.84	0.69	19.52	10.65	0.19	5.83	11.81	1.25	0.03	0.03	99.82	–0.31	41.7
P-45/2000	Golovnin Volcano	Quaternary	VF	62.13	0.74	15.22	8.79	0.17	3.05	6.84	2.19	0.46	0.04	99.65	2.48	4.8
P-62/2000	Golovnin Volcano	Quaternary	VF	65.60	0.61	16.64	6.55	0.14	1.86	5.23	2.65	0.33	0.06	99.67	3.33	8.1
P-79/8	Mendeleev Volcano	Quaternary	VF	60.83	1.11	15.28	10.42	0.13	3.78	5.41	2.70	0.19	0.08	99.93	4.76	14.2

Sample No.	Location	Age	Suite	Ba	Cr	Ga	Ni	Pb	Rb	Sc	Sr	V	Y	Zr
				[Trace elements in ppm]										
P-127/3	Kompressornii–Prasolova	Mid Miocene	RA	151	248	17.1	80.7	6.7	3.3	40	194	328	23.5	58
P-127/6	Kompressornii–Prasolova	Mid Miocene	RA	201	86	15.5	40.8	2.0	9.3	34	211	297	22.5	66
P-152/1	Orlovskii Ness	Mid Miocene	RA	403	19	14.9	3.5	3.3	18.2	12	195	31	27.6	116
P-174/4	Prasolovo–Nazarovo	Mid Miocene	RA	223	60	8.9	24.2	0.8	8.7	43	268	263	9.3	32
P-33/2	Prasolovo–Nazarovo	Mid Miocene	RA	98	77	14.4	20.4	5.4	5.8	46	266	408	23.1	69
P-74/4	Kompressornii–Prasolova	Mid Miocene	RA	146	17	16.5	12.4	4.5	7.3	43	181	393	19.0	50
P-75/13	Nazarovo–Lagunnoe Bay	Mid Miocene	RA	467	182	10.4	58.2	2.9	15.4	45	105	250	9.2	26
P-82/2	Prasolovo–Nazarovo	Mid Miocene	RA	255	53	11.2	15.9	5.5	15.2	33	256	223	21.7	73
P-82/3	Prasolovo–Nazarovo	Mid Miocene	RA	96	12	15.4	2.1	4.7	4.8	44	220	316	34.4	75
P-82/4	Prasolovo–Nazarovo	Mid Miocene	RA	218	147	12.1	27.6	4.2	5.2	38	175	319	27.8	69
P-61/4	Lovtsova peninsula	Mid Miocene	VF	37	14.6	3.9	0.0	0.0	5.3	56	141	329	13.5	27
P-54/2	Filatova Bay	Mid Miocene	VF	140	11	15.3	8.8	2.4	10.3	18	170	39	37.3	189
P-otp	Filatova Bay	Mid Miocene	VF	172	13	13.9	2.5	2.7	2.5	11	134	19	38.4	136
P-124/12	Ekaterina Volcano	Upper Miocene	RA	405	92	13.2	13.2	10.8	13.1	36	307	256	25.6	86
P-129/11	Prasolovo–Nazarovo	Upper Miocene	RA	278	61	12.4	18.1	–0.2	3.7	42	264	312	11.4	46
P-135/10	Nazarovo–Lagunnoe Bay	Upper Miocene	RA	245	24	14.8	6.8	5.3	11.6	38	359	415	13.0	35
P-135/6	Nazarovo–Lagunnoe Bay	Upper Miocene	RA	596	10	16.2	2.4	6.6	21.9	21	203	45	35.1	121
P-136/16	Nazarovo–Lagunnoe Bay	Upper Miocene	RA	226	102	11.1	35.1	1.7	14.9	32	197	200	28.4	103

P-138/2	Nazarovo–Lagunnoe Bay	Upper Miocene	RA	324	21	16.8	4.1	11.1	17.4	20	271	106	24.8	89
P-70/1	Ekaterina Volcano	Upper Miocene	RA	678	34	18.0	14.8	5.1	45.2	29	327	291	21.6	71
P-71/3	Ekaterina Volcano	Upper Miocene	RA	242	49	7.6	17.2	4.7	12.1	32	301	296	16.3	60
P-75/10	Kompressornii–Prasolova	Upper Miocene	RA	299	38	15.6	16.8	4.8	22.5	30	305	232	27.3	102
P-75/7	Kompressornii–Prasolova	Upper Miocene	RA	433	33	14.6	5.8	7.4	23.0	25	273	193	24.7	94
P-82/6	Nazarovo–Lagunnoe Bay	Upper Miocene	RA	126	106	16.9	33.3	5.8	5.1	34	254	261	19.5	53
P-147/25	Filatova Bay	Upper Miocene	VF	194	12	14.2	3.0	5.8	6.4	39	264	376	19.6	49
P-148/8	Filatova Bay	Upper Miocene	VF	101	69	13.9	16.0	3.6	2.7	39	222	280	16.0	29
P-51/3	Filatova Bay	Upper Miocene	VF	150	74	15.9	4.2	7.2	6.3	21	178	30	42.8	93
P-78/3	Mendeleev Volcano	Upper Miocene	VF	123	6	15.7	4.8	3.4	4.5	21	138	63	39.0	76
P-120/8	Ekaterina Volcano	Pliocene	RA	238	32	17.6	13.7	3.5	6.6	28	463	279	22.5	71
P-121/2	Ekaterina Volcano	Pliocene	RA	140	135	15.6	26.9	4.6	6.5	44	394	346	32.1	45
P-122/1	Ekaterina Volcano	Pliocene	RA	416	25	15.1	9.6	7.8	8.4	27	434	230	26.8	96
P-68/3	Ekaterina Volcano	Pliocene	RA	134	84	13.3	35.1	1.9	11.1	48	418	327	32.8	55
P-69/10	Ekaterina Volcano	Pliocene	RA	143	15	18.1	12.4	5.1	9.5	33	402	297	22.7	73
P-69/7	Ekaterina Volcano	Pliocene	RA	561	21	16.1	7.4	15.4	23.9	24	308	170	28.7	114
P-11/2003	Mendeleev Volcano	Pliocene	VF	194	8	13.9	5.0	7.8	9.4	32	170	174	26.7	64
P-151/1	Mostovaya–Filatova Bay	Pliocene	VF	116	46	15.0	10.8	4.2	6.0	43	216	273	16.8	42
P-151/6	Mostovaya–Filatova Bay	Pliocene	VF	24	104	13.9	17.5	2.2	2.2	45	256	254	10.5	26
P-84/2	Mostovaya–Filatova Bay	Pliocene	VF	132	54	16.0	13.4	5.5	6.2	37	228	226	19.2	49
P-112/14	Nazarovo–Lagunnoe Bay	Quaternary	RA	99	492	6.5	165.0	1.6	3.7	38	178	246	11.6	30
P-118/2000	Mendeleev Volcano	Quaternary	VF	186	4	15.9	3.8	5.4	8.8	27	245	98	30.2	66
P-191/2002	Mendeleev Volcano	Quaternary	VF	193	16	16.2	8.4	7.8	10.1	28	241	86	29.9	68
P-2/2003	Mendeleev Volcano	Quaternary	VF	286	38	14.1	3.3	10.8	13.0	28	213	114	37.7	101
P-202/2002	Mendeleev Volcano	Quaternary	VF	127	34	14.4	3.9	7.1	5.0	17	180	14	41.3	91
P-228/2001	Mendeleev Volcano	Quaternary	VF	290	7	14.8	4.0	11.8	11.1	28	218	138	24.6	100
P-241/2001	Mendeleev Volcano	Quaternary	VF	116	6	16.2	1.4	7.7	5.0	42	279	136	22.9	45
P-250/2001	Mendeleev Volcano	Quaternary	VF	253	0	19.4	7.6	7.3	6.3	38	334	79	81.9	69
P-258/2001	Mendeleev Volcano	Quaternary	VF	149	5	18.5	6.5	6.0	5.4	36	288	111	29.5	57
P-286/2001	Golovnin Volcano	Quaternary	VF	215	14	13.5	6.6	7.5	6.7	31	184	171	23.7	61
P-287/2001	Golovnin Volcano	Quaternary	VF	221	4	15.4	4.0	10.0	3.3	23	211	61	27.7	78
P-40/2000	Golovnin Volcano	Quaternary	VF	93	65	13.9	21.4	3.0	1.9	40	207	260	17.0	37
P-41/2000	Golovnin Volcano	Quaternary	VF	60	89	14.4	31.8	2.7	1.3	42	211	278	11.0	23
P-45/2000	Golovnin Volcano	Quaternary	VF	203	11	14.6	7.8	5.3	8.1	36	172	236	24.3	60
P-62/2000	Golovnin Volcano	Quaternary	VF	244	12	16.3	2.6	6.6	3.8	28	170	130	20.5	66
P-79/8	Mendeleev Volcano	Quaternary	VF	75	0	16.3	2.8	5.9	3.9	46	172	251	24.9	42

Fe is reported as Fe_2O_3; LOI, loss on ignition; RA, rear-arc; VF, volcanic front.

Table 2 Ultra-trace element and isotope compositions of selected Kunashir basalt to basaltic andesite lavas

Sample No.	P-82/3	P-61/4	P-135/10	P-120/8	P-68/3	P-69/10	P-151/6	P-112/14	P-228/2001	P-41/2000	P-127/6	P-75/13
Age	Mid Miocene	Mid Miocene	Upper Miocene	Pliocene	Pliocene	Pliocene	Pliocene	Quaternary	Quaternary	Quaternary	Mid Miocene	Mid Miocene
Suite	RA	VF	RA	RA	RA	RA	VF	RA	VF	VF	RA	RA
LOI in wt.%	6.94	9.68	0.67	1.85	2.51	5.29	1.85	–0.43	2.58	–0.31	2.54	1.85
SiO_2	54.13	53.23	50.14	53.60	50.15	52.89	49.36	48.95	64.97	49.84	51.26	52.50
[Ultra-trace elements in ppm]												
Li	7.60	6.66	3.90	4.77	8.29	5.54	2.32	2.72	5.05	3.66	–	–
Be	0.639	0.208	0.266	0.803	0.458	0.513	0.192	0.154	0.466	0.126	–	–
Rb	3.64	4.45	12.23	5.85	9.87	7.81	1.03	1.38	12.31	1.66	–	–
Y	31.3	12.8	14.7	23.5	35.7	19.6	11.7	11.1	26.4	11.3	–	–
Zr	65.7	27.61	4.7	63.9	62.1	69.7	22.2	20.3	120	17.1	–	–
Nb	1.173	0.250	0.328	1.524	2.115	1.320	0.231	0.243	1.083	0.116	–	–
Sb	0.284	0.156	0.110	2.048	0.049	0.516	0.105	0.037	0.239	0.091	–	–
Cs	0.31	0.317	0.99	0.79	0.48	2.42	0.04	0.08	0.78	0.12	–	–
La	7.16	1.117	2.77	9.35	11.32	8.12	1.61	1.94	5.62	0.95	–	–
Ce	18.92	3.913	6.80	23.66	18.07	20.21	4.13	4.42	15.16	2.85	–	–
Pr	2.59	0.658	1.02	2.99	3.41	2.56	0.70	0.78	2.22	0.50	–	–
Nd	12.84	3.853	5.09	15.32	17.46	11.41	3.55	3.60	10.77	2.81	–	–
Sm	4.06	1.534	1.70	3.74	4.58	3.12	1.28	1.24	3.29	1.08	–	–
Eu	1.50	0.834	0.76	1.28	1.54	1.07	0.51	0.53	1.24	0.48	–	–
Gd	5.89	2.201	2.16	4.33	6.23	3.76	1.77	1.88	4.05	1.59	–	–
Tb	1.04	0.401	0.38	0.68	1.08	0.68	0.33	0.34	0.71	0.30	–	–
Dy	6.63	2.754	2.51	4.47	6.29	4.00	2.22	2.09	4.78	2.07	–	–
Ho	1.28	0.588	0.54	0.93	1.28	0.76	0.49	0.45	0.97	0.46	–	–
Er	3.67	1.645	1.47	2.61	3.51	2.23	1.37	1.26	2.74	1.29	–	–
Tm	0.540	0.267	0.230	0.413	0.512	0.331	0.210	0.200	0.436	0.203	–	–
Yb	3.67	1.832	1.49	2.72	3.29	2.33	1.48	1.31	2.84	1.37	–	–
Lu	0.56	0.282	0.23	0.42	0.54	0.35	0.22	0.20	0.42	0.21	–	–
Hf	2.30	1.063	0.29	2.17	1.65	1.89	0.68	0.76	3.49	0.61	–	–
Ta	0.078	0.013	0.026	0.138	0.138	0.089	0.020	0.020	0.089	0.012	–	–
Tl	0.041	0.010	0.070	0.103	0.047	0.108	0.009	0.008	0.069	0.003	–	–
Pb	4.12	2.476	6.46	3.78	3.25	4.33	3.24	2.11	10.71	1.69	–	–
Th	1.47	0.148	0.34	2.05	1.28	1.85	0.20	0.42	1.66	0.08	–	–
U	0.468	0.454	0.083	0.653	0.516	0.544	0.094	0.134	0.629	0.037	–	–
[Isotopic ratios]												
$^{87}Sr/^{86}Sr$	0.704322	0.704417	0.703559	0.703285	0.703431	0.703601	0.703573	0.703445	0.703517	0.703458	0.703561	0.704727
2SE	0.000015	0.000015	0.000015	0.000015	0.000015	0.000015	0.000015	0.000015	0.000015	0.000015	0.000015	0.000016
$^{143}Nd/^{144}Nd$	0.513019	0.513141	0.513046	0.512993	0.512965	0.512995	0.513018	0.513012	0.513053	0.513085	0.512979	0.512925
2SE	0.000009	0.000010	0.000009	0.000009	0.000009	0.000009	0.000009	0.000009	0.000009	0.000009	0.000009	0.000009
$^{206}Pb/^{204}Pb$	18.3659	18.3864	18.3992	18.3675	18.3588	18.2858	18.4215	18.4218	18.3947	18.4175	18.3069	18.1981
2SE	0.0007	0.0007	0.0007	0.0007	0.0007	0.0008	0.0008	0.0008	0.0008	0.0007	0.0007	0.0007
$^{207}Pb/^{204}Pb$	15.5387	15.5373	15.5267	15.5281	15.5395	15.5435	15.5247	15.5278	15.5198	15.5224	15.5170	15.5068
2SE	0.0008	0.0007	0.0007	0.0007	0.0007	0.0007	0.0007	0.0008	0.0007	0.0008	0.0007	0.0007
$^{208}Pb/^{204}Pb$	38.3139	38.2897	38.2870	38.2872	38.3182	38.2245	38.3091	38.2908	38.2570	38.2641	38.2090	38.1037
2SE	0.0023	0.0018	0.0018	0.0021	0.0019	0.0017	0.0018	0.0020	0.0018	0.0021	0.0021	0.0020

–, not analyzed; 2SE, two standard error; RA, rear-arc; VF, volcanic front.

classification criteria are used throughout this paper. The VF/RA variation in the Quaternary lava is unclear in the case of Kunashir because the width of the volcanic arc is narrower than that in the North Zone (fig. 1 of Ishikawa & Tera 1997). One early Quaternary sample is from the RA area (locality 3 in Fig. 1c). However, it possesses clear VF features along with other Quaternary lavas as shown in the later sections. However, VF/RA variation occurs in the older Kunashir lavas; therefore, we apply the VF/RA distinction in this paper.

In terms of $Na_2O + K_2O$ *vs* SiO_2 (Fig. 2a), most of the Kunashir lavas are basalt to andesite, with lesser amounts of dacite and rhyolite; all are classified as sub-alkaline (Le Maitre *et al.* 1989). The VF lavas of all ages tend to plot in the lower total alkali region, although there is slight overlap between the VF and RA fields. All but one of the Quaternary lavas examined in this study are limited to the VF suite, and all fall in the lower sub-alkali region, which also includes one RA sample. In this meaning, there is no significant across-arc variation found in the Quaternary. All the Middle and Upper Miocene and Pliocene VF lavas fall in the same low alkali field as the Quaternary VF lavas, so that total alkalis along the VF area remain unchanged with time. Total alkali contents of the Miocene to Pliocene RA lavas generally plot near the sub-alkalic to alkalic transition, although one Pliocene RA lava has a low value.

Levels of K_2O in Kunashir lavas range continuously from low-K_2O to medium-K_2O varieties. The Middle Miocene, Upper Miocene, and Pliocene lavas show broad across-arc variation with K_2O contents increasing to the RA. Samples from VF plot in the low-K field, whereas those from the RA fall in the high low-K to low medium-K fields (Le Maitre *et al.* 1989; Fig. 2b). The Quaternary lavas from our collection are all characterized by low K content similar to total alkalis. Such across-arc variation in K_2O is comparable to variations observed elsewhere in the Kurile Arc ranging from almost zero up to greater than 2 wt% (Ryan *et al.* 1995; Bailey 1996). In contrast, the lavas from North Hokkaido in Miocene to Pliocene ages show no systematic across-arc variation in K_2O or $Na_2O + K_2O$; all of these have an RA affinity of Kunashir lavas of the same ages (Fig. 2).

The Middle Miocene, Upper Miocene, Pliocene lavas from Kunashir Island vary widely in MgO content (Fig. 3a). The Middle Miocene lavas have the highest MgO, up to 12.5 wt%. MgO contents fall steeply in basalt to basaltic andesite compositions with increasing SiO_2. The rocks from North Hokkaido show less variation overall, but maximum contents also reach 12.5 wt%. TiO_2 contents decrease with increasing SiO_2 and show no clear contrast between the VF and the RA over a time span of more than 15 Ma (Fig. 3b). The VF lavas also have greater Al_2O_3, CaO, and FeO*, and lesser Na_2O contents than the RA lavas (Fig. 3c–f). The North Hokkaido lavas have similar contents of Al_2O_3, but exhibit a vertical trend with slight variation in SiO_2.

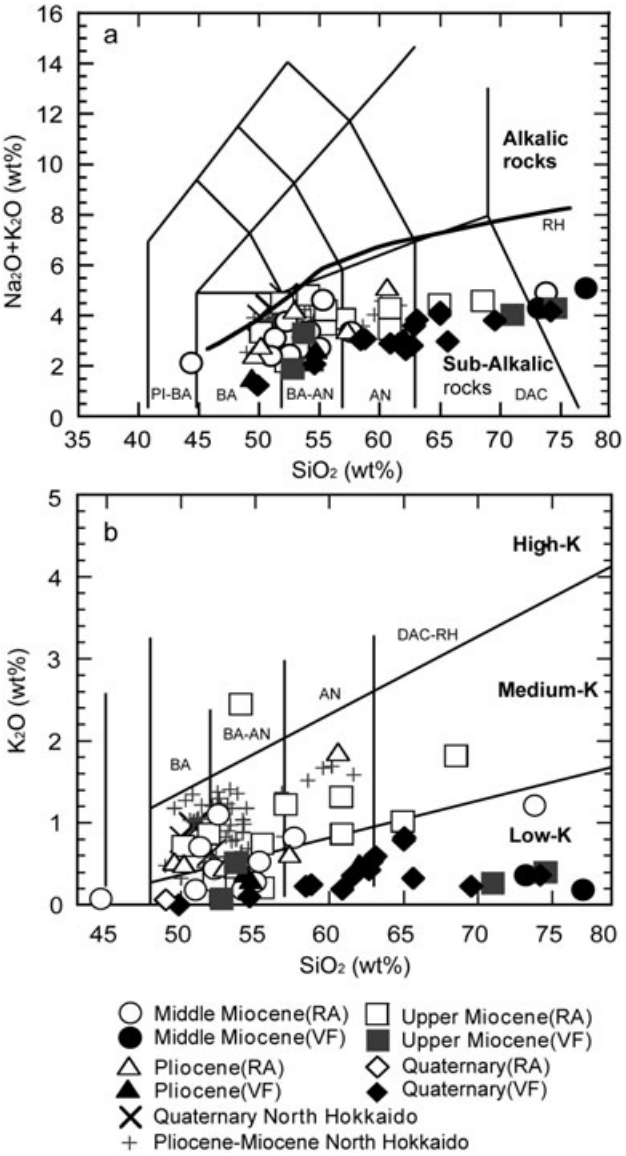

Fig. 2 SiO_2 *vs* (a) $Na_2O + K_2O$ and (b) K_2O plots (adapted from Le Maitre *et al.* 1989) for Kunashir lavas. Comparison to North Hokkaido lavas (Shuto *et al.* 2004) is also shown. RA, rear-arc; VF, volcanic front; PI-BA: picritic basalt; BA, basalt; BA-AN, basaltic andesite; AN, andesite; DA-RH, rhyo-dacite; RH, rhyolite. Open symbols, RA; closed symbols, VF. VF–RA criteria are based on physiographical distribution of the lava samples relative to the Quaternary volcanic front line shown in Fig. 1c.

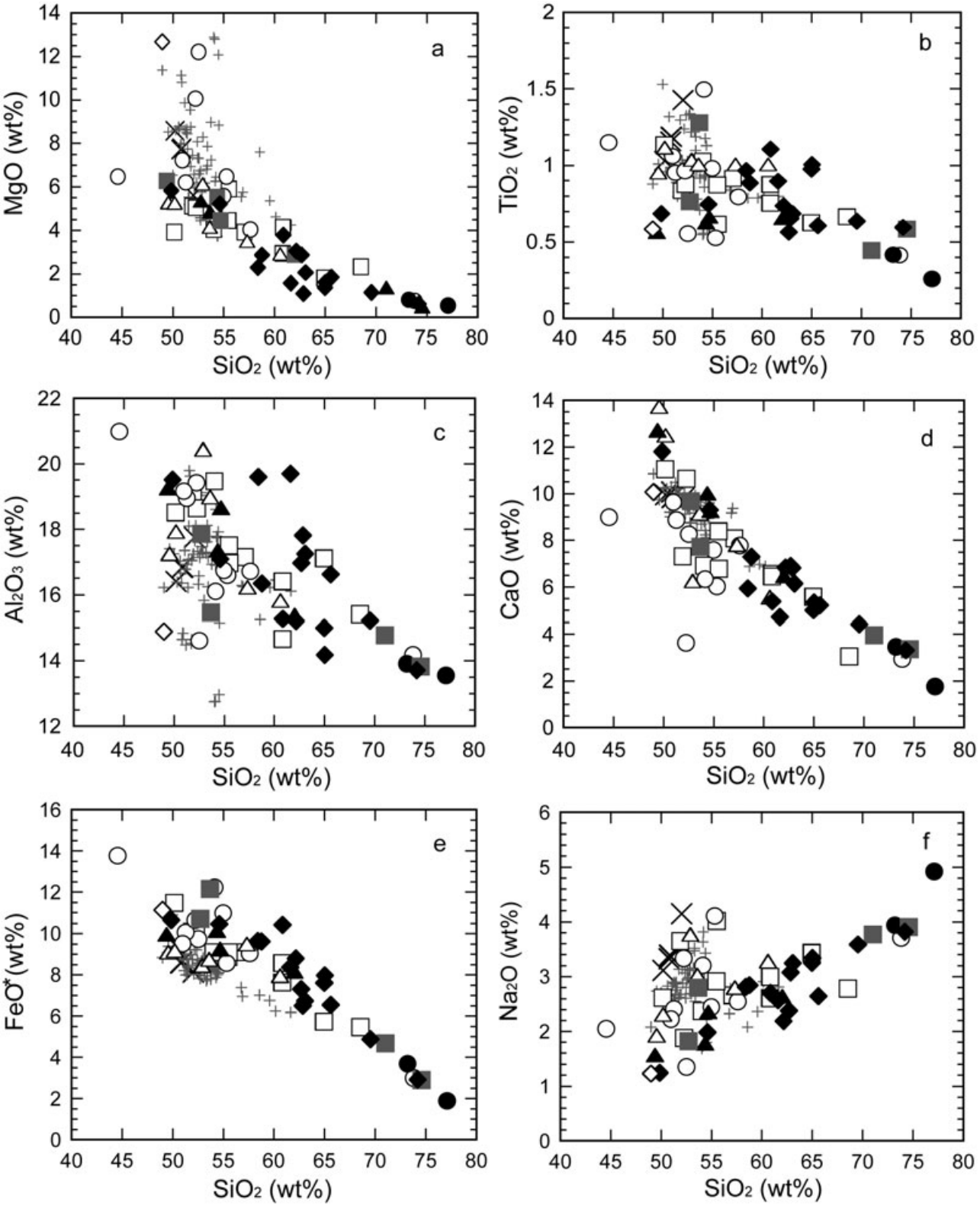

Fig. 3 Major element variation diagrams for Kunashir (this study) and North Hokkaido lavas (Shuto *et al.* 2004). RA, rear-arc; VF, volcanic front. Symbols as shown in Figure 2.

Contents of Rb, Ba, and Zr are particularly low in the VF lavas in Kunashir Island compared to those in the RA lavas (Fig. 4a–c). Maximum concentrations of Rb and Ba in the RA lavas are about two to three times greater than those in the VF, indicating similar behavior with total alkalis or K_2O among the major elements. In contrast to these elements, Y abundances are identical between the VF and RA, or between lavas of different age (Fig. 4e). The behavior of Sr is similar to Al_2O_3 (Fig. 4d). Chromium contents drop sharply in basalt to basaltic andesite suites, and the trend flattens out in andesite to dacite (Fig. 4f), showing similar behavior to MgO. The concentrations of elements such as Rb, Sr, and Cr in North Hokkaido lavas are greater than in Kunashir Island (Fig. 4a,d,f).

RARE EARTH AND ULTRA-TRACE ELEMENTS

The Kunashir lavas are characterized by relative enrichment of the primitive mantle (Sun & McDonough 1989) in Cs, Rb, Ba, U, Pb and Sr and low concentrations of Nb, Ta, and light rare earth element (LREE) (Fig. 5). Depletion in Nb and Ta relative to REE, and Sr and Pb enrichment are typical of subduction zone lavas, and all the Kunashir basalts possess these characteristics. The most depleted basalt occurs in the Quaternary VF. The Pliocene VF lava also has similar element concentrations, whereas the Pliocene RA basalts have elevated elemental abundances with or without Ba positive spikes. The Middle Miocene and Upper Miocene RA lavas generally have elevated trace element abundances, almost identical to the element concentrations of the Pliocene RA lavas.

Sr–Nd–Pb ISOTOPES

The range in Sr isotope compositions of Kunashir lavas is nearly identical for both the VF and RA, with an $^{87}Sr/^{86}Sr$ range 0.7033–0.7037 (Table 2; Fig. 6a). Three Middle Miocene lavas are exceptions, with $^{87}Sr/^{86}Sr > 0.7043$. These differing ratios may be due to seawater alteration judging from subaqueous emplacement and subsequent alteration (see LOI in Table 1). The same pattern of distribution of Sr and Nd isotopes is seen for samples from North Hokkaido. The Quaternary Kunashir basalts have slightly radiogenic $^{143}Nd/^{144}Nd$ compared to other basalts (Fig. 6a). The Sr and Nd isotope compositions are similar to those reported from the Indian Ocean mid-oceanic ridge basalts (MORBs) rather than the Pacific MORBs (Fig. 6a).

Isotope ratio plots such as $^{207}Pb/^{204}Pb$ *vs* $^{206}Pb/^{204}Pb$, $^{208}Pb/^{204}Pb$ *vs* $^{206}Pb/^{204}Pb$ (Fig. 6b,d) plot to the radiogenic side of the Indian MORB fields, distinct from ratios for Pacific MORB (Hochstaedter *et al.* 2001; not shown) The VF basalts plot at the most radiogenic end, whereas RA basalts are less radiogenic. This is maintained over the time range from Middle Miocene to the Quaternary age and the overall trend forms linear arrays (Fig. 6c,d). The same is true in the $^{143}Nd/^{144}Nd$ *vs* $^{206}Pb/^{204}Pb$ plot (Fig. 6c) suggesting a binary mixing covariation of Nd and Pb in magma genesis.

Overall, across-arc variation found in the lavas on Kunashir Island compares well with the across-arc geochemical variation reported in the Kurile Arc (Ryan *et al.* 1995; Bailey 1996; Bindeman & Bailey 1999). The across-arc variation includes an increase in total alkalis, K, Rb, Ba, Zr, Nb, Ta, and LREE to RA, whereas there is a decrease to RA in Pb/Ce, Sr/Nd, suggesting overall enrichment in large ion lithophile elements (LILEs) and high field strength elements (HFSEs) to the RA with some exceptions such as Pb and Sr. Such variations are commonly found in the Quaternary Kurile lavas (Ryan *et al.* 1995; Bailey 1996; Bindeman & Bailey 1999) indicating that Pb and Sr behave similarly to B and Sb as suggested by previous works. An increase in $^{143}Nd/^{144}Nd$ to the VF is also a common feature (Bindeman & Bailey 1999); Sr isotopes did not covary, perhaps due to seawater alteration in the case of the old subaqueous Kunashir lavas (Fig. 6a).

The RA feature is more prominent in the Middle Miocene lavas on Kunashir, VF/RA variation was apparent in Upper Miocene and Pliocene lavas as opposed to the Quaternary lavas, which possess a VF feature alone. There appears to have been a gross temporal development in the lava geochemistry of Kunashir; however, differences may be due to sampling bias originating from limited preservation of old fresh lavas. We hereafter examine the geochemical variation and its origin.

DISCUSSION

NEGLIGIBLE EFFECT OF CRUSTAL CONTAMINATION

Crustal or subcontinental lithosphere (SCLM) contamination has been considered by many

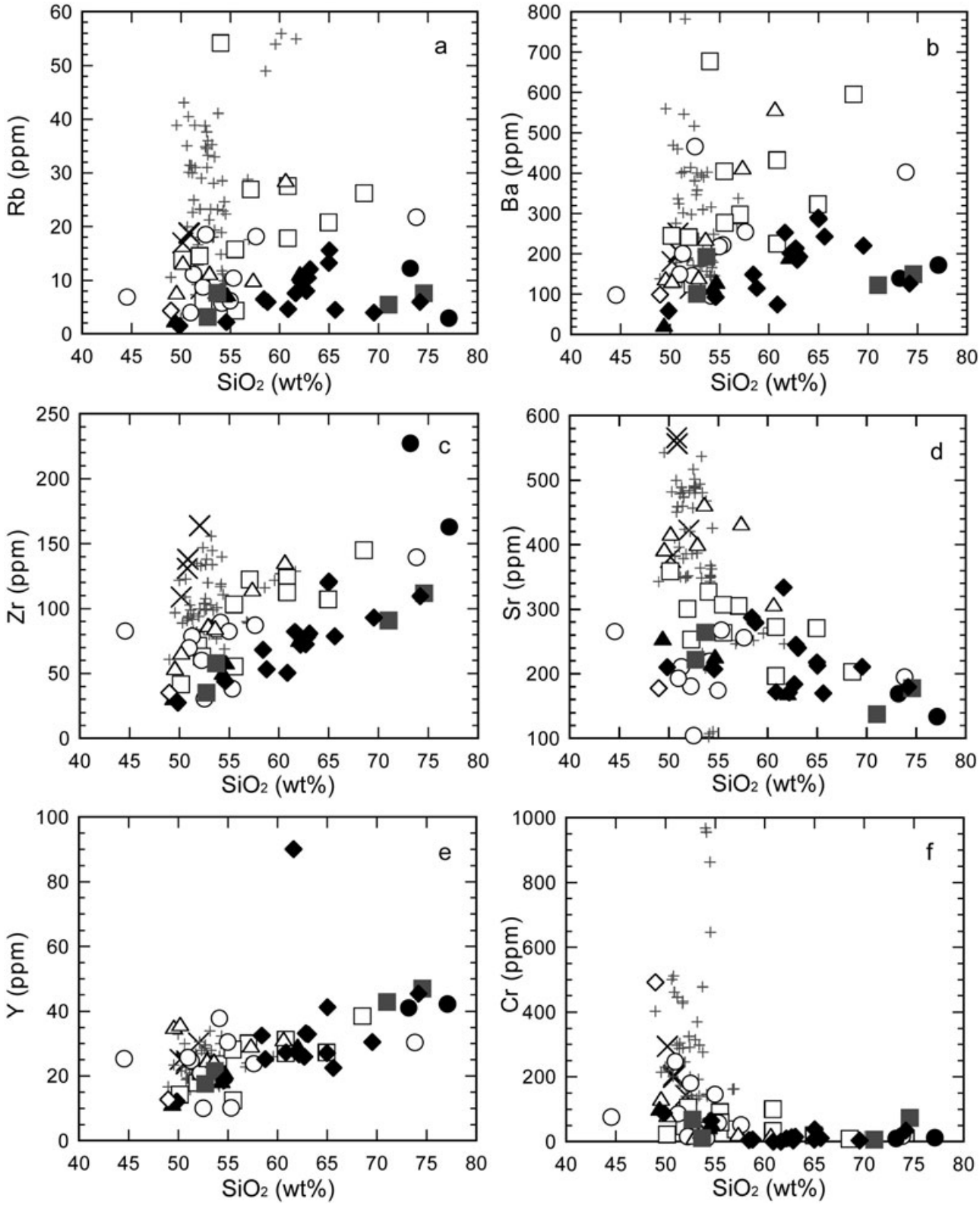

Fig. 4 Trace element variation diagrams for Kunashir and North Hokkaido lavas (Shuto *et al.* 2004). RA, rear-arc; VF, volcanic front. Symbols as shown in Figure 2.

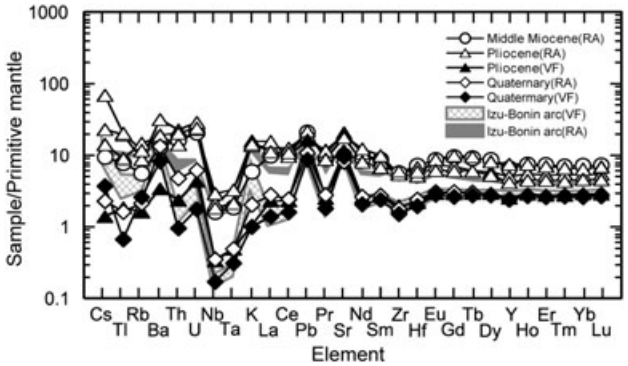

Fig. 5 Primitive mantle (Sun & McDonough 1989) normalized trace element patterns for lavas from Kunashir Island compared to Izu–Bonin Arc lavas (J.-I. Kimura, unpubl. data, 2008). RA, rear-arc; VF, volcanic front.

researchers to be an important factor for the geochemical diversity of island arc volcanic rocks (Gill 1981; Kersting *et al.* 1996; Kimura & Yoshida 2006); however, this factor seems to be insignificant in the South Zone Kurile basalts. On the $^{143}Nd/^{144}Nd$ *vs* SiO_2 diagram (Fig. 7), the Quaternary VF lavas from Kunashir Island plot on a horizontal line, increasing silica without change in Nd isotope ratios. This suggests no contamination during fractional crystallization (FC trend in Fig. 7), whereas basalts to basaltic andesites in the Pliocene and the Miocene Kunashir samples plot on a steeply vertical trend (Fig. 7). If progressive contamination affects lava chemistry during fractional crystallization, then the trend should be diagonal as shown by the AFC trend (Fig. 7). However, the vertical trend in the RA lavas would suggest contamination of less radiogenic Nd in the basalt source (Source Contamination trend in Fig. 7; also see discussions in Shuto *et al.* 2004 for Hokkaido).

ROLE OF SUBDUCTION COMPONENT

High LILE contents with HFSE depletion suggest the involvement of subduction components in the genesis of lavas on Kurile Islands (Ryan *et al.* 1995; Bindeman & Bailey 1999). Subduction fluid appears to have a predominant role in magma genesis, with sources constituting more than 95% of the altered ocean crust and less than 5% constituting oceanic sediment. (Ishikawa & Tera 1997).

Across the Kurile Arc, geochemical variations have been the key to interpreting the role of slab inputs. The fundamental characteristics are increasing from the VF to the RA in LILEs (K, Rb, Ba, partially Sr and Cs), REEs (La, Ce, Pr, Nd, Sm, Eu, Gd, Tb, Dy, Ho, Er, Tm, Yb, Lu) and HFSEs (Th, U, Nb, Ta, Zr, Hf, partially Y and Ti) (Ryan *et al.* 1995; Bindeman & Bailey 1999; this paper). An inverse relationship is seen in volatile elements such as B and Pb, and halogens such as F and Cl (Ryan *et al.* 1995; Bindeman & Bailey 1999), which is best displayed by B/Nb (Ishikawa & Tera 1997). A similar relationship is seen in this study, as Pb/Ce decreases from the VF to the RA (Fig. 5 shown by Pb spike relative to Ce). The overall increase in incompatible elements has been interpreted as a result of a lowering degree of partial melting to the RA. However, the decrease of highly volatile elements is interpreted as a result of the decrease in fluid flux liberated from the slab from the VF to the RA (Ishikawa & Nakamura 1994; Ryan *et al.* 1995; Bindeman & Bailey 1999).

Covariation between isotopes and element abundances is also common. Decreasing radiogenic Nd with increasing radiogenic Sr to the RA (Bindeman & Bailey 1999) or increasing $\delta^{11}B$ with increasing radiogenic Sr to the RA (Ishikawa & Tera 1997) have been reported. Our isotopic data reproduced increasing radiogenic Nd to the VF (Fig. 6a), but failed to reproduce Sr behavior due to seawater alteration in old samples (see above). Our Pb isotope data indicate an increase in radiogenic Pb in VF lavas but less radiogenic Pb in the RA lavas. This appears to contradict a previous study (Bindeman & Bailey 1999); however, their work did not specifically address across-arc variation in Pb isotopes (see their figure 7). Our Pb isotope ratios, in contrast, correlate linearly to the Nd isotope ratios (Fig. 6b), and thus, clearly show across-arc variation.

There are multiple controlling factors on the arc basalt genesis, although the contribution of slab flux is of common importance. In the case of the Kurile Arc, the contribution of slab derived fluid is ascribed by consensus, as enrichment in highly fluid-mobile elements including Pb and B. Their strong slab derived isotope signatures (high $\delta^{11}B$ and radiogenic Pb) are clearly correlated to the element enrichment in VF lavas. An increase in alkalinity correlates well to the LILE, HFSE, and REE enrichment (see above sections), indicating decreases in the degree of melting to the RA although the element ratios or abundances do not always follow the melting degree scheme (e.g. Kimura & Yoshida 2006).

The reasons for high abundance of incompatible elements in the RA lavas of the Kurile Arc

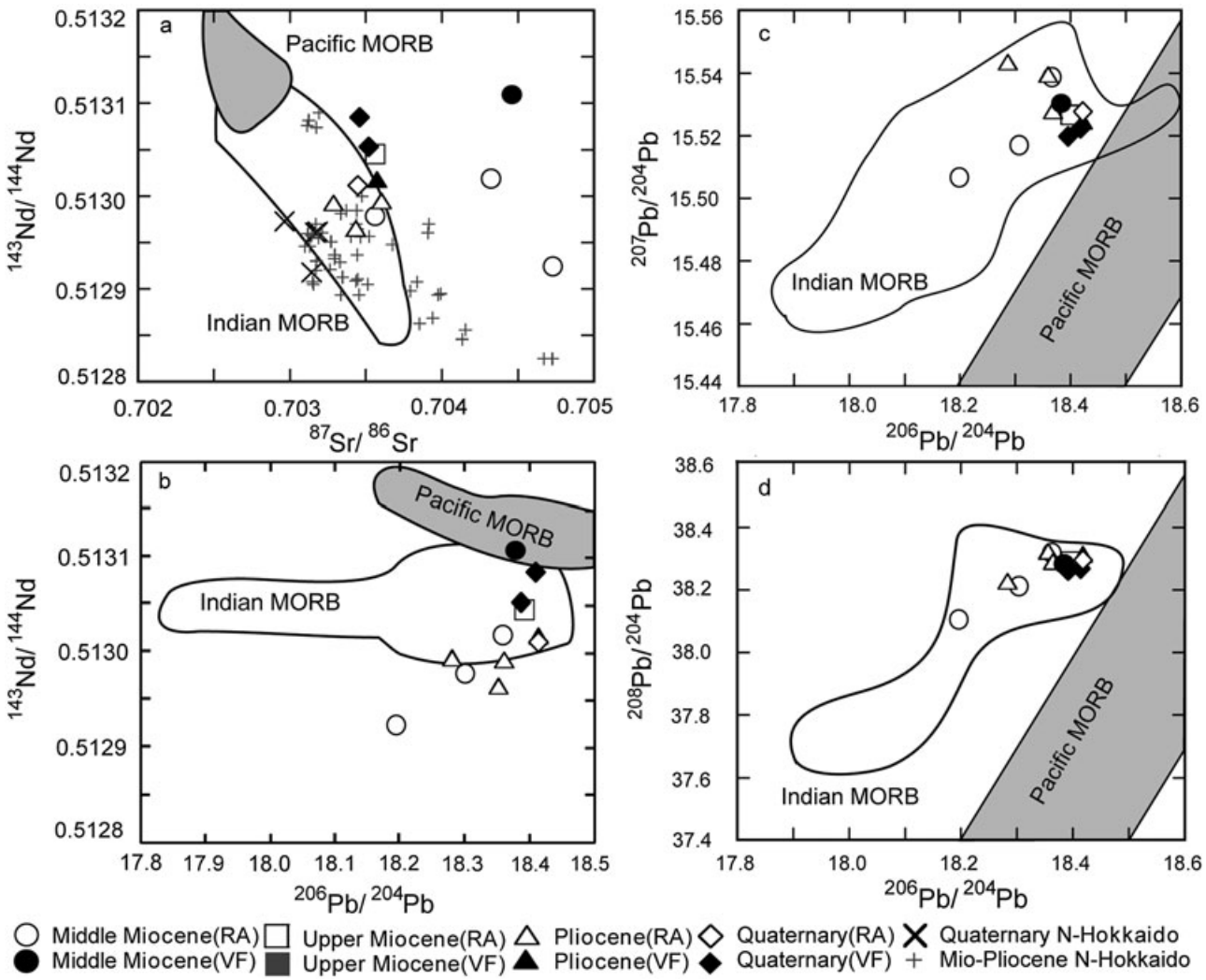

Fig. 6 Isotope ratio diagrams showing (a) $^{87}Sr/^{86}Sr$ *vs* $^{143}Nd/^{144}Nd$, (b) $^{206}Pb/^{204}Pb$ *vs* $^{207}Pb/^{204}Pb$ (c) $^{206}Pb/^{204}Pb$ *vs* $^{143}Nd/^{144}Nd$, (d) $^{206}Pb/^{204}Pb$ *vs* $^{208}Pb/^{204}Pb$ for lavas from Kunashir Island. Data source for Pacific and Indian MORB in (a,c) (Kimura & Yoshida 2006); Pacific MORB in (b,d) (Taylor & Nesbitt 1998), Indian MORB in (b,d) (Durpé & Allègre 1983; Hamelin & Allègre 1985; Rehkämper & Hofmann 1997). RA, rear-arc; VF, volcanic front.

basalt are disputed. This geochemical feature may originate: (i) simply from low degrees of melting; (ii) from the contribution of deep fluids released by the breakdown of particular hydrous mineral phases such as phlogopite or phengite in metasomatized mantle or dehydrated slab; or (iii) from the contribution of slab melt (Ryan *et al.* 1995; Ishikawa & Tera 1997). The contribution of slab components is also a source of debate; whether sediment (SED) or MORB altered oceanic crust (AOC) is the major contributor of the slab fluid or melt and at what ratios. For example, a large role of slab derived fluid to the VF has been suggested by B–Sr isotope systematics (Ishikawa & Tera 1997) with 95% fluid derived from AOC plus 5% from SED components.

We here examine geochemical discrimination diagrams that have been applied to reveal contributions of altered AOC and SED fluids as well as SED melts or bulk sediments in arc magma genesis. These methods are based on different behaviors of elements during slab dehydration or melting (Kogiso *et al.* 1997; Johnson & Plank 1999; Kessel *et al.* 2005) combined with elemental abundances or radiogenic isotopes (Plank & Langmuir 1993; Hauff *et al.* 2003; Kimura & Yoshida 2006).

We first examine the diagram $^{143}Nd/^{144}Nd$ *vs* Th/Nd (Fig. 8). The AOC and AOC fluid end members used are the same with those discussed in Ishizuka *et al.* (2006b). Sediment fluid and sediment melt compositions are calculated based on bulk composition of the SED column subducting into the Kurile and Japan Island Arc systems (Plank & Langmuir 1998). The bulk distribution coefficients between sediment and fluid (700°C)

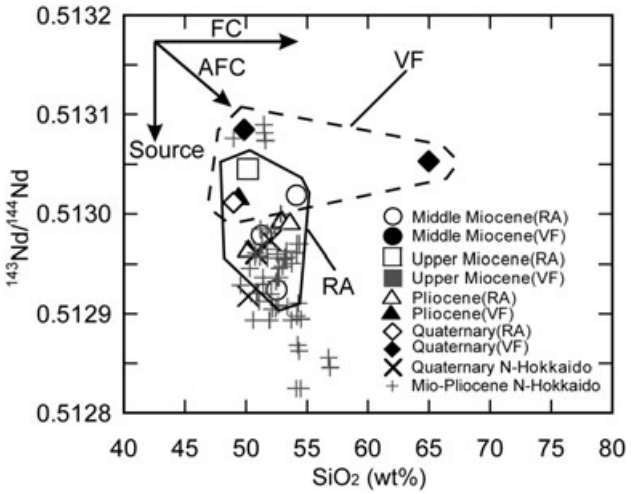

Fig. 7 $^{143}Nd/^{144}Nd$ *vs* SiO_2 plot for Kunashir lavas to test the role of contamination. AFC, assimilation and fractional crystallization; FC, fractional crystallization; RA, rear-arc; VF, volcanic front.

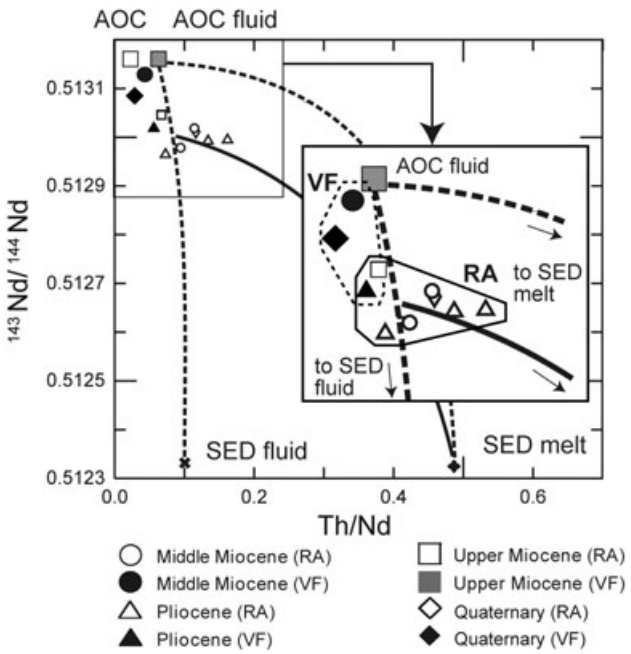

Fig. 8 Th/Nd *vs* $^{143}Nd/^{144}Nd$ plot for Kunashir lavas and relationship to the slab components. The altered oceanic crust MORB (AOC) and AOC fluid end members are the same as used in Ishizuka *et al.* (2006b). Sediment (SED) fluid and sediment melt components were calculated based on averaged bulk composition of sediment columns subducted at trenches of the Kurile and Japan Island Arc systems (Plank & Langmuir 1998). Bulk distribution coefficients between sediment and fluid (700°C) and sediment and melt (900°C) are from Johnson and Plank (1999). RA, rear-arc; VF, volcanic front.

and sediment and melt (900°C) are from Johnson and Plank (1999). There are significant uncertainties in the evaluation of subcontinental mantle chemical composition beneath the Kurile Arc. We have followed the method proposed by Tatsumi (2003) and assume that the mantle wedge composition is similar to depleted mantle composition, which should have a similar Nd isotope ratio and Th/Nd as AOC. Th and Nd are highly incompatible elements and the Th/Nd ratio is not significantly affected by melting or fractional crystallization processes (e.g. Pertermann *et al.* 2004) even in hydrous melting conditions (Green *et al.* 2000). They are both fluid-immobile (e.g. Johnson & Plank 1999) and Th is more readily incorporated into sediment melt than Nd because of the high concentration of Th in sediment. Consequently, Th/Nd can be used diagnostically to distinguish between hydrous fluid and melt involvement in basalt magma genesis in subduction zones. (e.g. Plank & Langmuir 1993). On the $^{143}Nd/^{144}Nd$ *vs* Th/Nd diagram (Fig. 8) the VF samples lie on a mixing line between AOC and SED fluids. Evidence of a relatively small contribution from SED fluid is consistent with the conclusion based on B–Sr isotope systematics reported by Ishikawa and Tera (1997). The same mixture proportion (~95% fluid derived from AOC plus ~5% from SED components) was calculated for the frontal arc basalt lavas of the Izu–Bonin Arc (Straub *et al.* 2004).

On the same diagram, the RA lavas are characterized by higher Th/Nd with lower $^{143}Nd/^{144}Nd$, forming a flat array (Fig. 8). The variation can be accounted for if a small proportion of SED melt contributed to the source along with AOC and SED fluids. Note that we used all VF/RA lavas analyzed, including Middle Miocene to Quaternary lavas, because all have clear VF/RA characteristics comparable to other Quaternary Kurile lavas.

Such a relationship is also observed in a Nd isotope *vs* Nb/Zr plot, on which similar quasilinear correlations are evident in VF (vertical) and in RA (orthogonal) (Fig. 9). Nb/Zr is a HFSE ratio that is relatively conservative against low temperature and seawater alteration, and thus, is suitable for magma source examination. This element ratio can be fractionated by partial melting of mantle peridotite when garnet is involved (Green 1995). However, the partition coefficient driven element fractionation can not correlate to Nd isotope ratios. Moreover, any low pressure slab fluids can not transfer the low Nb/Zr character from SED to the mantle melting region, due to the very low mobility of these elements in fluid (Kessel *et al.* 2005). Instead, slab melts or high-pressure supercritical fluids can transfer the low Nb/Ta characteristics from the slab source, due to high element

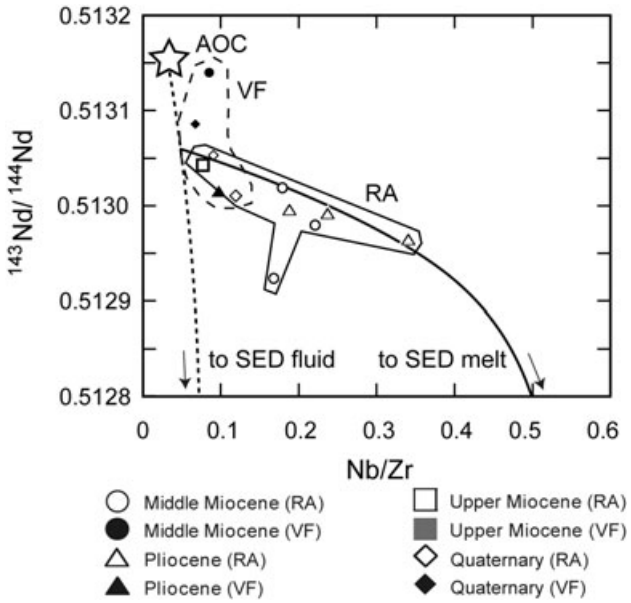

Fig. 9 Nb/Zr *vs* $^{143}Nd/^{144}Nd$ plot for the Kunashir lavas. Mixing lines between altered oceanic crust MORB (AOC) fluid and sediment (SED) fluid and SED melt are drawn arbitrarily because experimental results of Johnson and Plank (1999) did not give bulk Zr partition coefficients. Others are in the same scheme with Figure 8. Increase in Zr/Nb covarying with Nd isotope composition in the RA basalts is not explained by any processes other than binary mixing to SED melt having low Nd isotope ratio and high Nb/Zr. ☆, AOC; RA, rear-arc; VF, volcanic front.

solubility in the melts/supercritical fluids (Aizawa *et al.* 2004; Kessel *et al.* 2005). In addition, Nd is also effectively transferred by the melt/supercritical fluids (Kessel *et al.* 2005). Correlation between $^{143}Nd/^{144}Nd$ and Nb/Zr (Fig. 9) strongly suggests that involvement of a slab SED component greatly affected the RA basalt source, as has been suggested by previous works in the Izu and northeast Japan Arcs (Ishizuka *et al.* 2006b; Kimura & Yoshida 2006). This diagram also supports the above conclusion that the slab components influencing the Kurile lavas appear to be a mixture between AOC fluid and SED fluid/melt (Fig. 8).

We prefer an explanation involving the addition of slab SED melt–supercritical fluid in the RA basalt source (e.g. Ishizuka *et al.* 2006b, 2007) rather than the transfer of slab components via fluids captured in mica minerals (phengite or phlogopite) and later release by a pressure dependent breakdown of these phases beneath the RA. These minerals can retain K, Rb, and Ba but not Nd and Th (Green *et al.* 2000; Green & Adam 2003). Covariation between Nd isotope and HFSEs and Th is better explained by melting of slab SED component at RA depth (perhaps > 150 km = 5 GPa). Alternatively, a high-pressure fluid can behave supercritically and dissolve large amount of ions including HFSEs and REEs (Kessel *et al.* 2005). Therefore, it is possible the SED melt component can also be supplied by such form.

The remaining issue is the positive correlation between Pb and Nd isotopes (Fig. 6b). An increase in SED melt component can decrease radiogenic Nd but would increase radiogenic Pb as well. This appears to be inconsistent with the fact that more radiogenic Pb in found in VF lavas. The correlation between Pb and Nd isotopes, however, can be explained by a greater contribution of mantle melts at smaller degrees of partial melting beneath RA. This may be evidenced by the non-significant spike in Pb relative to Nd in the RA basalts, suggesting less Pb addition from the slab component to the RA basalt source (Fig. 5). According to this, a lower degree of melting in the RA mantle should also be one cause of the high incompatible element abundances in the RA lavas and partially control isotope behaviors in the Kurile Arc system. A mass balance approach will solve the issue; however, this is beyond the scope of this paper.

CONCLUSIONS

Middle Miocene, Upper Miocene, Pliocene, and Quaternary lavas from Kunashir Island in the South Zone of the Kurile Arc show characteristic across-arc geochemical variations. The Kunashir lavas possess oceanic arc characteristics, and are basically unaffected by enriched continental materials such as crust or SCLM. Incompatible trace element and Sr–Nd–Pb isotope compositions suggest that the VF and the RA lavas are affected by both AOC and SED slab components, with greater SED melt–supercritical fluid contribution to the RA lavas. The SED slab component also affects HFSE (e.g. Nb/Zr) in the lavas, indicating transfer of the component from the slab via melt or supercritical fluid. The effect of enriched SCLM and continental materials is greater in the northeast Japan Arc and is significant in northeastern Hokkaido; however, this effect is not prominent on Kunashir Island. This magma generation system appears to have been maintained from the middle Miocene through to the present with increasing VF signature over the time. This provides an interesting insight into the tectonic history of the Kurile Basin BAB opening and development of the Kurile Arc.

ACKNOWLEDGEMENTS

Reviews by Drs J. Ryan and B. Dryer and editorial handling by Dr Y. Tamura were extremely helpful in improving the draft manuscript. We thank Dr B. P. Roser of Shimane University for supervising the XRF and for discussion. We are also grateful to Ms M. Katakuse and Mr Y. Shimoshioiri of Shimane University and to Mr A. A. Chashin and Mrs N. E. Gvozdeva of the Far East Geological Institute of Russian Academy of Science for help with preparation of the samples. This study was financially supported by a Japan Society for the Promotion of Science (JSPS) scholarship to A. Martynov for the Special Graduate Course program of Shimane University and by grant #07-05-00310 of the Russian Foundation of Fundamental Research.

REFERENCES

AIZAWA K., YOSHIMURA R. & OSHIMAN N. 2004. Splitting of the Philippine Sea Plate and a magma chamber beneath Mt. Fuji. *Geophysical Research Letters* **31**. Doi:10.1029/2004GL019477.

BAILEY J. C. 1996. Role of subducted sediments in the genesis of Kuril-Kamchatka island arc basalts: Sr isotopic and elemental evidence. *Geochemical Journal* **30**, 289–321.

BAILEY J. C., FROLOVA T. I. & BURIKOVA I. A. 1989. Mineralogy, geochemistry and petrogenesis of Kurile island-arc basalts. *Contributions to Mineralogy and Petrology* **102**, 265–80.

BARANOV B., WONG H. K., DOZOROVA K., KAPP B., LÜDMANN T. & KARNAUKH V. 2002. Opening geometry of the Kurile Basin (Okhotsk Sea) as inferred from structural data. *Island Arc* **11**, 206–19.

BINDEMAN I. N. & BAILEY J. C. 1999. Trace elements in anorthite megacrysts from the Kurile Island Arc: A window to across-arc geochemical variations in magma compositions. *Earth and Planetary Science Letters* **169**, 209–26.

DUPRÉ B. & ALLÈGRE C. J. 1983. Rb-Sr variation in Indian Ocean basalts and mixing phenomena. *Nature* **303**, 142–6.

FEDORCHENKO V. I., ABDURAHMANOV A. I. & RODIONOVA R. I. 1989. *Volcanism of the Kuril island arc: Geology and petrogenesis*. Nauka, Moscow.

GILL J. B. 1981. *Orogenic Andesites and Plate Tectonics*. Springer-Verlag, Heidelberg.

GORSHKOV G. S. 1967. *Volcanism of the Kuril island arc*. Nauka, Moscow.

GOTO Y., NAKAGAWA M. & WADA K. 1995. Tectonic setting of the Miocene volcanism in northern Hokkaido, Japan: Speculation from their K-Ar ages and major element chemistry. *Journal of Mineralogy Petrology and Economic Geology* **90**, 109–23.

GREEN T. H. 1995. Significance of Nb/Ta as an indicator of geochemical processes in the crust-mantle system. *Chemical Geology* **120**, 347–59.

GREEN T. H. & ADAM J. 2003. Experimentally determined trace element characteristics of aqueous fluid from partially dehydrated mafic oceanic crust at 3.0 GPa, 650–700°C. *European Journal of Mineralogy* **15**, 815–30.

GREEN T. H., BLUNDY J. D., ADAM J. & YAXLEY G. M. 2000. SIMS determination of trace element partition coefficients between garnet, clinopyroxene and hydrous basaltic liquids at 2–7.5 GPa and 1080–1200°C. *Lithos* **25**, 165–87.

HAMELIN B. & ALLÈGRE C. J. 1985. Large-scale regional units in the depleted upper mantle revealed by an isotope study of the South-West Indian Ridge. *Nature* **315**, 196–9.

HAUFF F., HOERNLE K. & SCHMIDT A. 2003. Sr–Nd–Pb composition of Mesozoic Pacific oceanic crust (Site 1149 and 801, ODP Leg 185): Implications for alteration of ocean crust and the input into the Izu-Bonin-Mariana subduction system. *Geochemistry Geophysics Geosystems (G3)* **4**. Doi:10.1029/2002GC000421.

HOCHSTAEDTER A., GILL J., PETERS R., BROUGHTON P. & HOLDEN P. 2001. Across-arc geochemical trends in the Izu-Bonin arc: Contributions from the subducting slab. *Geochemistry Geophysics Geosystems (G3)* **2**. Doi:10.1029/2000GC000105.

IIZUMI S., MAEHARA K., MORRIS P. A. & SAWADA Y. 1994. Sr isotope data of some GSJ rock reference samples. *Memoir of Faculty of Science, Shimane University* **28**, 83–6.

IIZUMI S., MORRIS P. A. & SAWADA Y. 1995. Nd isotope data for GSJ reference samples JB-1a, JB-3 and JG-1a and the La Jolla standard. *Memoir of Faculty of Science, Shimane University* **29**, 73–6.

ISHIKAWA T. & NAKAMURA E. 1994. Origin of the slab component in arc lavas from across-arc variation of B and Pb isotopes. *Nature* **370**, 205–8.

ISHIKAWA T. & TERA F. 1997. Source, composition and distribution of the fluid in the Kurile mantle wedge: Constraints from across-arc variations of Br/Nb and B isotopes. *Earth and Planetary Science Letters* **152**, 123–38.

ISHIZUKA O., KIMURA J.-I., LI Y. B. *et al.* 2006a. Early stages in the evolution of Izu-Bonin arc volcanism: New age, chemical, and isotopic constraints. *Earth and Planetary Science Letters* **250**, 385–401.

ISHIZUKA O., TAYLOR R. N., MILTON J. A., NESBITT R. W., YUASA M. & SAKAMOTO I. 2006b. Variation in the mantle sources of the northern Izu arc with time and space – Constraints from high-precision Pb isotopes. *Journal of Volcanology and Geothermal Research* **156**, 266–90.

ISHIZUKA O., TAYLOR R. N., YUASA M. *et al.* 2007. Processes controlling along-arc isotopic variation of the southern Izu-Bonin arc. *Geochemistry Geophysics Geosystems* **8**. Doi:10.1029/2006GC001475.

JOHNSON M. C. & PLANK T. 1999. Dehydration and melting experiments constrain the fate of subducted sediments. *Geochemistry Geophysics Geosystems (G3)* **13**. Doi:10.1029/999GC000014.

KELLEY K. A., PLANK T., GROVE T. L., STOLPER E. M., NEWMAN S. & HAURI E. 2006. Mantle melting as a function of water content beneath back-arc basins. *Journal of Geophysical Research* **111**. Doi:10.1029/2005JB003732.

KERSTING A. B., ARCULUS R. J. & GUST D. A. 1996. Lithospheric contributions to arc magmatism: Isotope variations along strike in Volcanoes of Honshu, Japan. *Science* **272**, 1464–8.

KESSEL R., SCHMIDT M. W., ULMER P. & PETTKE T. 2005. Trace element signature of subduction-zone fluids, melts and supercritical liquids at 120–180 km depth. *Nature* **439**, 724–7.

KIMURA G. 1996. Collision orogeny at arc-arc junctions in the Japanese islands. *Island Arc* **5**, 262–75.

KIMURA J.-I. & YAMADA Y. 1996. Evaluation of major and trace element XRF analyses using a flux to sample ratio of two to one glass beads. *Journal of Mineralogy, Petrology and Economic Geology* **91**, 62–72.

KIMURA J.-I. & YOSHIDA T. 2006. Contributions of slab fluid, mantle wedge and crust to the origin of Quaternary lavas in the NE Japan arc. *Journal of Petrology* **47**, 2185–232.

KIMURA J.-I., YOSHIDA T. & TAKAKU Y. 1995. Igneous rock analysis using ICP-MS with internal standardization, isobaric ion overlap correction, and standard addition methods. *Science Report of Fukushima University* **56**, 1–12.

KIMURA J.-I., KAWAHARA M. & IIZUMI S. 2003. Lead isotope analysis using TIMS following single column-single bead Pb separation. *Geoscience Report of Shimane University* **22**, 49–53.

KOGISO T., TATSUMI Y. & NAKANO S. 1997. Trace element transport during dehydration processes in the subducted oceanic crust: 1. Experiments and implications for the origin of oceanic island basalts. *Earth and Planetary Science Letters* **148**, 193–205.

LE MAITRE R. W., BATEMAN P., DUDEK A. *et al.* 1989. *A Classification of Igneous Rocks and Glossary of Terms*. Blackwell, Oxford.

MARTYNOV J. A., DRIL S. I., CHASHCHIN A. A., RYBIN A. V. & MARTYNOV A. J. U. 2005. Geochemistry of basalts of islands Kunashir and Iturup – A role non subducted factors in magma genesis, the Kuril island arc. *Geochemistry* **4**, 369–83.

MIYASHIRO A. 1974. Volcanic rock series in island arcs and active continental margins. *American Journal of Science* **274**, 321–55.

NAKAJIMA S., SHUTO K., KAGAMI H., OHKI J. & ITAYA T. 1995. Across-arc chemical and isotopic variation of Late Miocene to Pliocene volcanic rocks from the Northern Japan arc. *Memoir of the Geological Society of Japan* **44**, 197–226.

OKAMURA S., SUGAWARA M. & KAGAMI H. 1995. Origin and spatial variation of Miocene volcanic rocks from north Hokkaido, Japan. *Memoir of the Geological Society of Japan* **44**, 165–80.

OKAMURA S., ARCULUS R. J., MARTYNOV Y. A., KAGAMI H., YOSHIDA T. & KAWANO Y. 1998. Multiple magma sources involved in marginal-sea formation: Pb, Sr, and Nd isotopic evidences from the Japan Sea region. *Geology* **26**, 619–22.

OKAMURA S., ARCURUS R. J. & MARTYNOV Y. A. 2005. Cenozoic magmatism of the North-Eastern Eurasian Margin: The role of lithosphere versus asthenosphere. *Journal of Petrology* **46**, 221–53.

PEARCE J. A. & PARKINSON I. J. 1993. Trace element models for mantle melting: Application to volcanic arc petrogenesis. *In* Prichard H. M., Alabaster T., Harris N. B. W. & Neary C. R. (eds.) *Magmatic Processes and Plate Tectonics*, Geological Society, London, Special Publication **76**, 373–403.

PEATE D. W. & PEARCE J. A. 1998. Causes of spatial compositional variations in Mariana arc lavas: Trace element evidence. *Island Arc* **7**, 479–95.

PERTERMANN M., HIRSCHMANN M. M., HAMETNER K., GUNTHER D. & SCHMIDT M. W. 2004. Experimental determination of trace element partitioning between garnet and silica-rich liquid during anhydrous partial melting of MORB-like eclogite. *Geochemistry Geophysics Geosystems (G3)* **22**. Doi:10.1029/2003GC000638.

PISKUNOV B. N. 1987. Geological significance of volcanism of island arcs. Nauka, Moscow.

PLANK T. & LANGMUIR C. H. 1993. Tracing trace elements from sediment input to volcanic output at subduction zones. *Nature* **362**, 739–42.

PLANK T. & LANGMUIR C. H. 1998. The chemical composition of subducting sediment and its consequences for the crust and mantle. *Chemical Geology* **145**, 325–94.

POUCLET A. & BELLON H. 1992. Geochemistry and isotopic composition of volcanic rocks from the Yamato Basin: Hole 794D, Sea of Japan. *In* Tamaki K., Suyehiro K., Allan K. & McWilliams M. (eds.) *Proceedings of the Ocean Drilling Program, Scientific Results 127/128, Pt. 2*, pp. 779–89, Ocean Drilling Program, College Station, TX.

POUCLET A., LEE J.-S., VIDAL P., COUSENS B. & BELLON H. 1994. Cretaceous to Cenozoic volcanism in South Korea and in the Sea of Japan: Magmatic constraints on the opening of the back-arc basin. *In* Smellie J. L. (ed.) *Volcanism Associated with Extension at Consuming Plate Margins*, Geological Society, London, Special Publication **86**, 169–91.

REHKÄMPER M. & HOFMANN A. W. 1997. Recycled ocean crust and sediment in Indian Ocean MORB. *Earth and Planetary Science Letters* **147**, 93–106.

RYAN J. G., MORRIS J., TERA F., LEEMAN W. P. & TSVETKOV A. 1995. Cross-arc geochemical variations in the Kurile Arc as a function of slab depth. *Science* **270**, 625–7.

SATO M., SHUTO K. & YAGI M. 2007. Mixing of asthenospheric and lithospheric mantle-derived basalt magmas as shown by along-arc variation in Sr and Nd isotopic compositions of Early Miocene basalts from back-arc margin of the NE Japan arc. *Lithos* **96**, 453–74.

SHIBATA T. & NAKAMURA E. 1997. Across-arc variations of isotope and trace element compositions from Quaternary basaltic rocks in northeastern Japan: Implications for interaction between subducted oceanic slab and mantle wedge. *Journal of Geophysical Research* **102**, 8051–64.

SHUTO K., HIRAHARA Y., ISHIMOTO H., AOKI A., JINBO A. & GOTO Y. 2004. Sr and Nd isotopic compositions of the magma source beneath north Hokkaido, Japan: Comparison with the back-arc side in the NE Japan arc. *Journal of Volcanology and Geothermal Research* **134**, 57–75.

SHUTO K., ISHIMOTO H., HIRAHARA Y. *et al.* 2006. Geochemical secular variation of magma source during Early to Middle Miocene time in the Niigata area, NE Japan: Asthenospheric mantle upwelling during back-arc basin opening. *Lithos* **86**, 1–33.

STERN R. J. 2004. Subduction initiation: Spontaneous and induced. *Earth and Planetary Letters* **226**, 275–92.

STERN R. J. & BLOOMER S. H. 1992. Subduction zone infancy: Examples from the Eocene Izu-Bonin-Mariana and Jurassic California. *Geological Society of America Bulletin* **104**, 1621–36.

STRAUB S. M., LAYNE G. D., SCHMIDT A. & LANGMUIR C. H. 2004. Volcanic glasses at the Izu arc volcanic front: New perspectives on fluid and sediment melt recycling in subduction zones. *Geochemistry Geophysics Geosystems (G3)* **22**. Doi:10.1029/2002GC000408.

SUN S.-S. & MCDONOUGH W. F. 1989. Chemical and isotopic systematics of oceanic basalts: Implications for mantle composition and processes. *In* Saunders A. D. & Norry M. J. (eds.) *Magmatism in the Ocean Basins*, Geological Society, London, Special Publication **42**, 313–45.

SYRACUSE E. M. & ALBERS G. A. 2006. Global compilation of variations in slab depth beneath arc volcanoes and implications. *Geochemistry Geophysics Geosystems* **23**. Doi:10.1029/2005GC001045.

SYVOROTKIN V. L. & RUSINOVA S. V. P. 1989. Effusives of Kunashir Island-Fourth Formation upon the island arc. *In* Shumyatskaya T. N. (ed.) *Magmatism of Rift (Petrology, Evolution, Geodynamic)*, pp. 180–8. Nauka Publish House, Moskow.

TAKAGI T., ORIHASHI Y., NAITO K. & WATANABE Y. 1999. Petrology of a mantle-derived rhyolite, Hokkaido, Japan. *Chemical Geology* **160**, 425–45.

TAMAKI K., SUYEHIRO K., ALLAN J., INGLE J. C. & PISCIOTTO K. A. 1992. Tectonic synthesis and implications of Japan sea ODP Drilling. *In* Tamaki K., Suyehiro K., Allan J. *et al.* (eds.) *Proceedings of the Ocean Drilling Program, Scientific Results*, pp. 1333–48, Ocean Drilling Program, College Station, TX.

TARARIN I. A., LELIKOV E. P. & ITAYA T. 2000. Pleistocene submarine volcanoes of east part Kuril arc (sea of Okhotsk). *Reports of the Russian Academy of Science* **371**, 366–70.

TATSUMI Y. 2003. Some constrains on arc magma genesis. *In* Eiler J. (ed.) *Inside the Subduction Factory*. Geophysical Monograph, Vol. 138, pp. 277–92, American Geophysical Union, Washington, DC.

TAYLOR B. & MARTINEZ F. 2003. Back-arc basin basalt systematics. *Earth and Planetary Science Letters* **6632**, 1–17.

TAYLOR R. N. & NESBITT R. W. 1998. Isotopic characteristics of subduction fluids in an intra-oceanic setting, Izu-Bonin Arc. *Earth and Planetary Science Letters* **164**, 79–98.

YOSHIDA T. 2001. The evolution of arc magmatism in the NE Honshu arc, Japan. *Tohoku Geophysical Journal* **36**, 131–49.

YOSHIDA T., OHGUCHI T. & ABE T. 1995. Structure and evolution of source area of the Cenozoic volcanic rocks in Northeast Honshu arc, Japan. *Memoir of the Geological Society of Japan* **44**, 263–308.

ZHURAVLEV D. Z., TSVETKOV A. A. & ZHURAVLEV A. Z. 1985. Lateral variations of isotopic characteristics in Nd and Sr in Quaternary lavas of the Kuril island arc and their petrogenetic importance. *Geochemistry* **12**, 1723–36.

ZLOBIN T. K., PISKUNOV V. N. & FROLOV T. I. 1987. New data about structure of an earth's crust in the central part of the Kuril island arc. *Report of the Russian Academy of Science* **293**, 185–7.